Available online at www.CivileJournal.org

Civil Engineering Journal

Vol. 5, No. 12, December, 2019

Structural Characteristics of Developed Sustainable Lime-Straw Composite

Sajid Kamil Zemam [a*], Sa'ad Fahad Resan [a], Musab Sabah Abed [a]

[a] *Civil Engineering Department, Engineering College, University of Misan, Amarah, Iraq.*

Received 25 June 2019; Accepted 29 September 2019

Abstract

Construction materials made of renewable resources have promising potential given their low cost, availability, and environmental friendliness. Although hemp fibers are the most extensively used fiber in the eco-friendly building sector, their unavailability hinders their application in Iraq. This study aimed to overcome the absence of hemp fiber in Iraq and develop a new sustainable construction material, strawcrete, by using wheat straw and traditional lime as the base binder. A comparable method of developing hempcrete was established. The experimental program adopted novel Mixing Sequence Techniques (MSTs), which depended on changing the sequence of mixed material with fixed proportions. The orientation of the applied load and the specimen's aspect ratio were also studied. The mixing proportion was 4:1:1 (fiber/binder/water) by volume. Results showed that the developed strawcrete had a dry unit weight ranging from 645 kg/m3 to 734 kg/m^3 and a compressive strength ranging from 1.8 MPa to 3.8 MPa. The enhanced physical and strength properties varied with the MST and loading orientation. The properties of the developed hempcrete were compared with those of strawcrete.

Keywords: Hempcrete; Strawcrete; Wheat Straw Fiber; Mixing Sequence Technique; Compressive Strength; Loading Orientation; Strength Rating.

1. Introduction

In recent years, the tendency for designing low-environmental-impact buildings to meet the requirement of ecosystems has emphasized on the global use of bio-aggregate-based concretes. The term bio-aggregate concretes refers to the mixture of binders (lime, clay, plaster, and cement) and natural fibers (hemp, straw, flax, bamboo, and animal hairs) [1]. In this context, the use of eco-friendly concrete such as hempcrete [2], wood-concrete [3], papercrete [4], and mud-concrete [5] has been growing considerably. Hempcrete is most widely used in the field of green construction owing to its remarkable environmental quality as a non-CO_2 producer [6, 7]. Furthermore, walls made of hemp–lime composite exhibit better sound absorption and thermal isolation than conventional concrete walls [8]. Hempcrete had been introduced in the early 90s in France by using the matrix of lime and hemp shiv particles [9]. From the construction point of view, hempcrete, similar to several biomass concretes, is predominantly non-load bearing material; nevertheless, its strength is important to provide the solidity to hold its own weight [10, 11].

The strength of hempcrete significantly depends on the binder type, density, and morphology of hemp fiber. Hempcrete density varies with the applied tamping effort [12]. Four levels of densities are usually identified to be vary from very light density to high density [13]. Extensive research has been undertaken to determine the factors affecting hemp concrete strength. E. P. Aigbomian [14] stated that the compressive strength of hemp concrete varies with mixture

* Corresponding author: sajid.kamil@uomisan.edu.iq

http://dx.doi.org/10.28991/cej-2019-03091435

proportions from 0.02 MPa to 1.22 MPa. Moreover, the binder added with 10%–25% Portland cement can improve the compressive strength of hempcrete and increase its density [13]. Previous studies have focused on enhancing the mechanical properties of hempcrete by selecting the raw materials, percentage, and types of binders; furthermore, the importance of the applied tamping effort and particle size distribution of bio-aggregates has been highlighted [15]. Thus, hempcrete has paved the way for the utilization of agro-fiber in the construction industry. In many countries and in Iraq, hemp fiber is unavailable because of legal issues, thereby obstructing the use of hempcrete. Abundant agricultural by-products were adopted as alternatives to hemp fibers for use in the construction sector to overcome this issue. In this context, rice husk fiber was used as an alternative to hemp fiber to develop a new isolation building envelop [16].

Likewise, woodcrete was developed using sawdust and lime as base binder; woodcrete a new building material that is capable of withstanding loads similar to that hempcrete [14]. Growing attention has been directed to straw fiber as building materials in the past decades. In this context, straw bale building has significantly contributed to the design of low-carbon and energy-efficient building [13] given its thermal and acoustical advantages [17]. Straw fiber is usually a by-product of annual growing crops; thus, it is cheap and obtainable in most countries. Wheat is the major source of straw fiber. Iraq occupies the 31st position in global wheat production. The average wheat production in Iraq is 3,753,111 t from 2014 to 2016 [18]. Therefore, the use of straw fiber for building purposes provides a sustainable and ecological approach of recycling [14]. Reusing abundant wheat straw fiber in the present study as an alternative of hemp fiber for bio-concrete closes the gap of hemp absence in Iraq.

Discussion about the importance of mixing sequence and its influence on strength characteristics of bio-aggregate base concretes is few [9]. In this context, some authors suggested to preliminary blend water and binder in a pan mixer to produce a homogenous slurry; afterward, the bio-aggregate was added and further mixed until full uniformity was reached [15]. Other authors proposed a mix by pre-wetting the bio-aggregates, and lime-based binder was added subsequently [16]. All of the adopted sequences were undertaken as a mixing procedure without considering their effect on strength characteristics. Therefore, this paper first proposed straw fiber as an alternative to hemp and examined the significant influence of mixing sequence on the physico-mechanical properties of bio- aggregate-based concretes. Loading orientation with respect to tamping layer was also studied.

2. Experimental Program

The experimental work was performed at the Construction Laboratory of Engineering Faculty at Misan University. The main variables considered in this study were related to Mixing Sequence Techniques (MST), loading direction with respect to orientation of tamping layers, casting age effect, and sample aspect ratio.

2.1. Materials

Wheat straw fiber (WSF) was chosen as a bio-aggregate because of its abundant supply in Iraq. On the basis of previous research carried out on hemp shiv slices, fiber size (length) has been found as a function of density and strength [19]. Strawcrete, the straw fiber in this study, was used in its natural morphology to determine the effect of mixing sequence on the strength properties of the developed bio-aggregate. Furthermore, Joseph Williams stated that loading orientation does not depend on fiber size [15]. The fiber size distribution ranges from 5 mm to 50 mm as shown in Figure 1. Wheat straw has a number of uses as fuel, livestock bedding, feed, fodder, and in thatch making. In the construction sector, the use of WSF in Iraq has a historical value as a major additive for improving unfired clay building units called adobe [20] of ancient clay house. Locally available lime powder is used throughout this work as base binder in which it is conformed to BS 890 Class B [21]. Moreover, 50% of binder was included with ordinary Portland cement to gain extra strength for the developed bio-composite in this study as recommended by literature [13]. Chemical analysis and the main compounds of the used cement aside from the physical properties conformed to the Iraqi specification number (5/1984) [22] and in accordance with the ASTM C191 [23].

2.2. MSTs

The sequence of mixing in bio-aggregate concrete has not been specified until now. In the present study, two different sequences have been designed as shown in Figures 2 and 3. MST-I in Figure 2(a) represents the mixing sequence in which the binder has been pre-mixed with water to produce a semi-thick slurry and then added to the dry fiber. The materials were mixed gently. The casting of bio-composite materials requires a specific effort to ensure an acceptable density for the produced samples. MST-II in Figure 2(b) shows the mixing sequence in which the total water has been pre-mixed with dry straw fiber. Then, the binder was added in the form of powder and mixed together. The binder was mixed with wheat straw fiber with a fiber/binder ratio of 4:1 as recommended in previous studies [24]. Table 1 shows the material proportions for the two used techniques.

Figure 1. Straw fiber size distribution

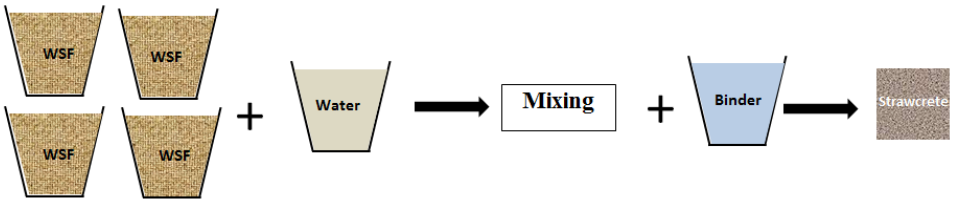

(a) MST-I

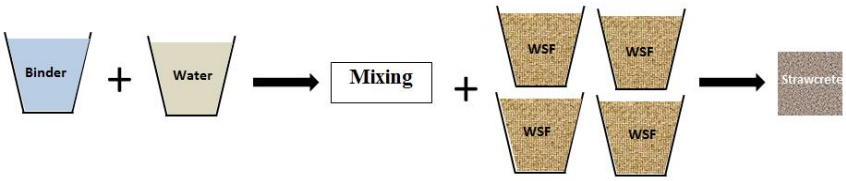

(b) MST-II

Figure 2. Mixing Sequence Techniques (MST)

(a) MST-I

(b) MST-II

Figure 3. Mixing procedure

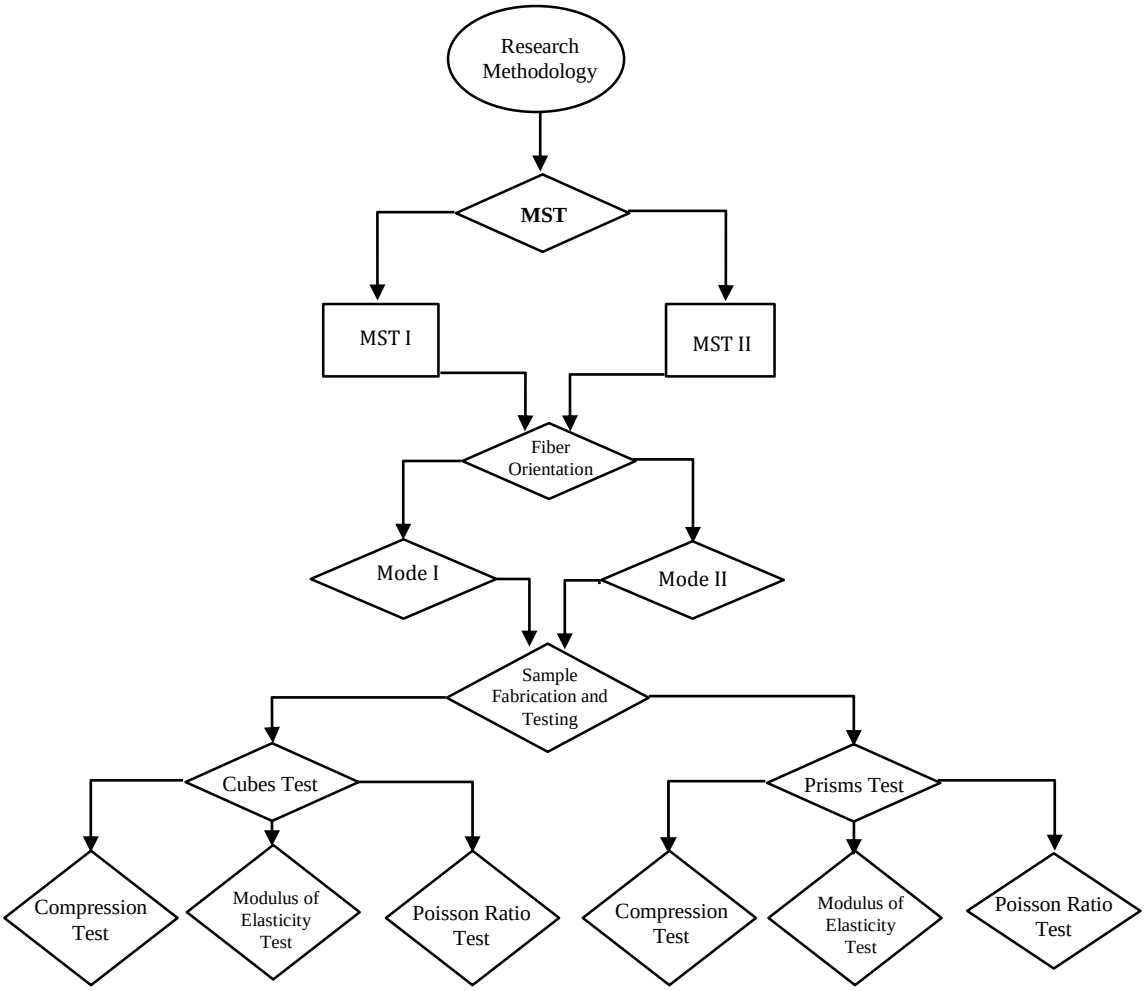

Figure 4. Flow chart of the research methodology

Table 1. Material proportions of the adopted mixes

No.	Designation	Mixing sequences	Lime kg/m^3	Cement kg/m^3	Binder kg/m^3	Water/binder ratio	Water kg/m^3	Wheat straw Binder ratio	Wheat straw fiber kg/m^3
1	MST-I	Binder–water–fiber	100	108	208	1:1.25	166	1:2.85*	73
2	MST-II	Fibre–water–binder							

2.3. Fiber Orientation and Loading Modes

The same compacted effort was used for both mixing techniques. The number of tamping for each layer was designed as 20 with three layers for each sample. The weight of the tamping tool was 2 kg, and the drop height was approximately 30 cm. Thus, the constant applied effort was 105 kN.m/m^3. The tamping direction forced wheat straw fibers within the matrix to be oriented to the plane of the tamped layers**.** As loading was applied in a specified orientation, we investigated two basic cases to the study matrix anisotropy. These were the loading normally applied to the tamping layer orientation (loading mode 1) and along it (loading mode 2). Figure 5 shows the configuration of the tamped layers and their respective loading modes**.**

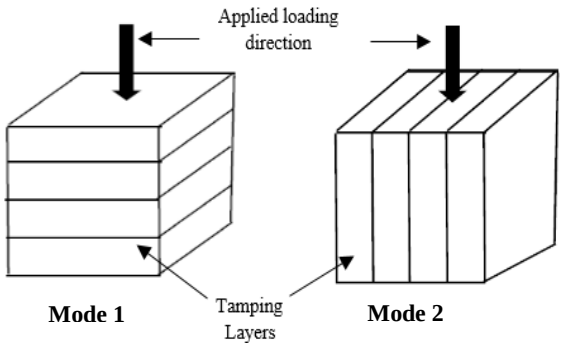

Figure 5. Configuration of the tamped layers and their respective loading modes

2.4. Sample Fabrication and Test Setting

Various compressive and flexural tested specimens were fabricated depending on the previously described mixing techniques and tested in the assigned two different loading modes. The duration of specimen testing was 56 days. A compression machine (ELE) was used to test the specimens for compressibility, whereas a 10 t hydraulic jack was used for flexural tested specimens. Testing load is usually directly applied using a relatively rigid steel plate at a maintained constant rate of 10 kg/s by using equal increments at each step. The mechanical dial gauges with accuracy of 0.01 mm were placed to measure the specimen's deformation, whereas applied loading was recorded using a calibrated load cell. Figures 6 and 7 show the fabricated specimens and described test arrangement. The compression specimens were encoded using a simplified designation, "ABCi" as follows:

- Denoted aspect ratio, S for cubes and P for prisms
- Denoted applied loading direction, N for mode 1 and P for mode 2
- Denoted mixing sequence technique, T1 for MST-I and T2 for MST-II

Figure 6. Fabricated specimens

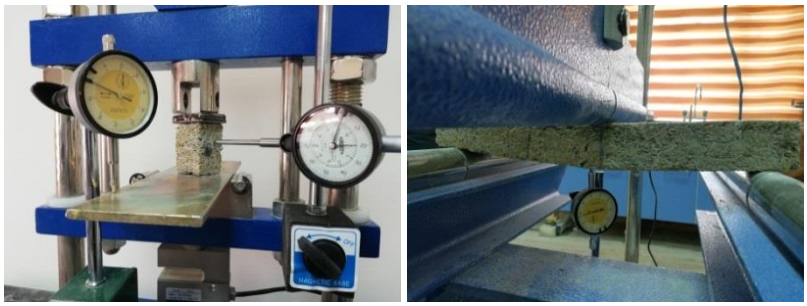

Figure 7. Test arrangement

3. Results and Discussion

The experimental results of various specimens related to the two adopted matrices showed that although these matrices had the same material proportions and tampering efforts, the specific mixing method or specific wheat fiber orientation affected their mechanical properties and structural performance. Table 3 shows the mechanical and structural characteristics of the developed strawcrete specimens discussed throughout this study. The mechanical properties and structural characteristics of the developed strawcrete specimens with different MSTs and WSF orientation are listed in Table 1. The specimens fabricated using MST-II with the fiber orientation mode 1 exhibited high compressive strength (3.8 MPa), fracture strength (0.69 MPa), and flexural capacity (4.66 MPa). The corresponding compressive strength rating (2.83 MPa) and flexural strength rating (4.4) maintained high ratings among others as the unit weight was slightly affected by the mixing technique. The bulk density changed from 645 kg/m^3 to 734 kg/m^3. For various mixing techniques or fiber orientation, high-strength specimens exhibited softening behavior assigned by the modulus of elasticity dropping. Specimen compressibility, which could be indicated by Poisson ratios, confirmed the fiber orientation mode 1 as a matrix of high compressibility. The assigned negative Poisson ratio could be affected by large out-of-plane buckled layers within the matrix of fiber orientation 2. The modulus of elasticity usually increased as the Poisson ratio decreased, thereby resulting in extreme anisotropy. Poisson ratio, ν, and elastic modulus, E, of different specimens are summarized in Table 2.

Table 2. Structural characteristics of the developed strawcrete specimens

Group	MST	Bulk Density, kg/m^3	WSF Orientation	Modulus of Elasticity, MPa	Poisson Ratio, N	Compressive Strength, MPa	Compressive Strength Rating	Fracture Strength, MPa	Flexural Capacity, kN.m	Flexural Strength Rating
1	MST-I	645	Mode1	7.1	0.053	1.8	1.94	0.22	1.49	1.6
2			Mode2	10.54	0.029	0.34	0.37	0.09	0.61	0.656
3	MST-II	734	Mode1	10	0.07	3.8	2.83	0.690	4.66	4.40
4			Mode2	14.84	0.04	0.697	1.66	0.288	1.94	1.83

3.1. MST Effects

The second-adopted MST (MST-II) was assigned as the most efficient proper technique because for the same loading orientation (normal to tamping layers), the compression strength of the specimens prepared using MST-II were 3.8 MPa (for SNT2) against 1.8 MPa (for SNT1) and was prepared via MST-I. Figure 8 shows the stress–strain trending in the scope of the MST effect. Figure 9 shows the loading–time trending in terms of the MST effect. For the loading orientation distinguished using parallel to tamping layers, the stress–strain behavior shows a ductile behavior in comparison with the normal mode with humble compression strength although the specimens prepared using MST-II were advancing in developing strength. Figures 10, shows the stress–strain trending of MST effects in the scope of tamping orient mode 2.

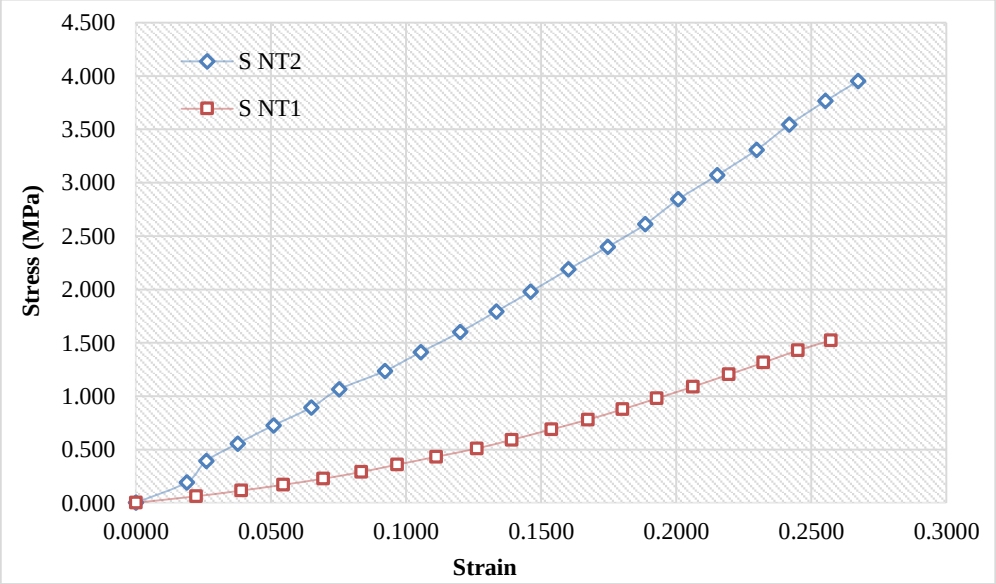

Figure 8. Stress - strain trending in the scope of MST effect

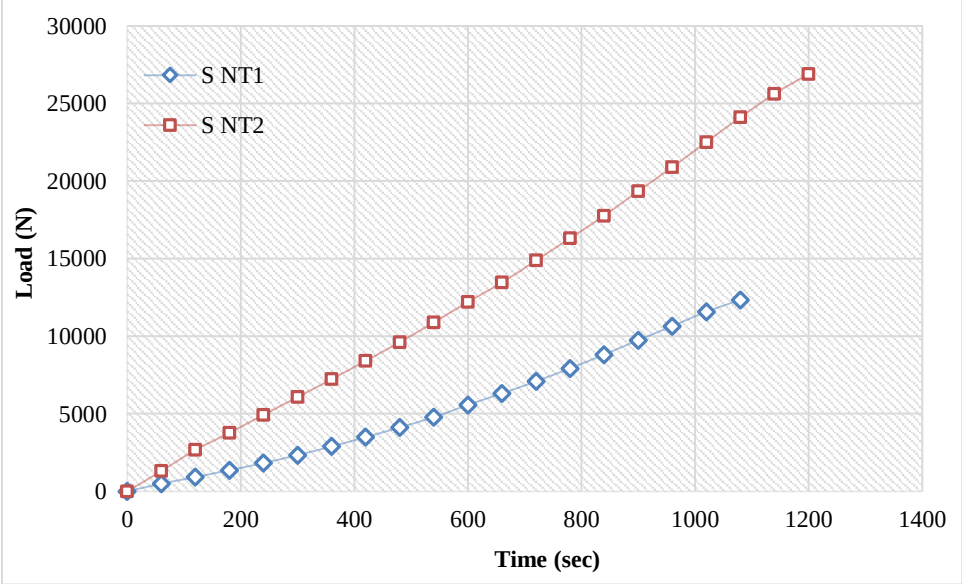

Figure 9. Loading–time trending in scope of the MST effect

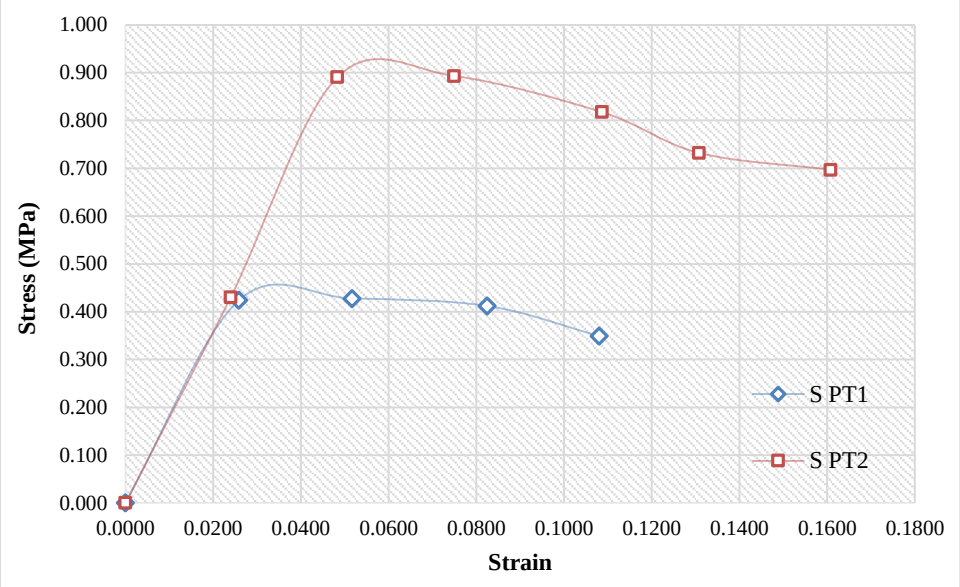

Figure 10. Stress–strain trending of MST effect in scope of tamping orient mode 2

3.2. Fiber Orientation and Loading Mode Effect

Two distinguished loading methods were considered in this study. In the first method, one load was applied normally to the tamping layers, and the second one was applied along the tamping layers. The normal mode was assigned as the excellent mode to utilize the full strength capacity of the developed matrix. For the same sequence technique, the compression strength dropped from 3.8 MPa to 0.9 MPa as the loading mode changed from normal to parallel. Figure 11 shows the stress–strain trend in the scope of the tamping orientation effect in which the specimens subjected to loading parallel to tamping layout exhibited comprehensive mechanically softer response than those undergoing normal loading mode (mode 1). Sensitizing the tamping layer orientation for the applied loading direction highly affected the stress concentration within and around the bonded layers; these layers dominated the elasticity of the entire matrix and resulted in similar plates buckling along the specimen's depth.

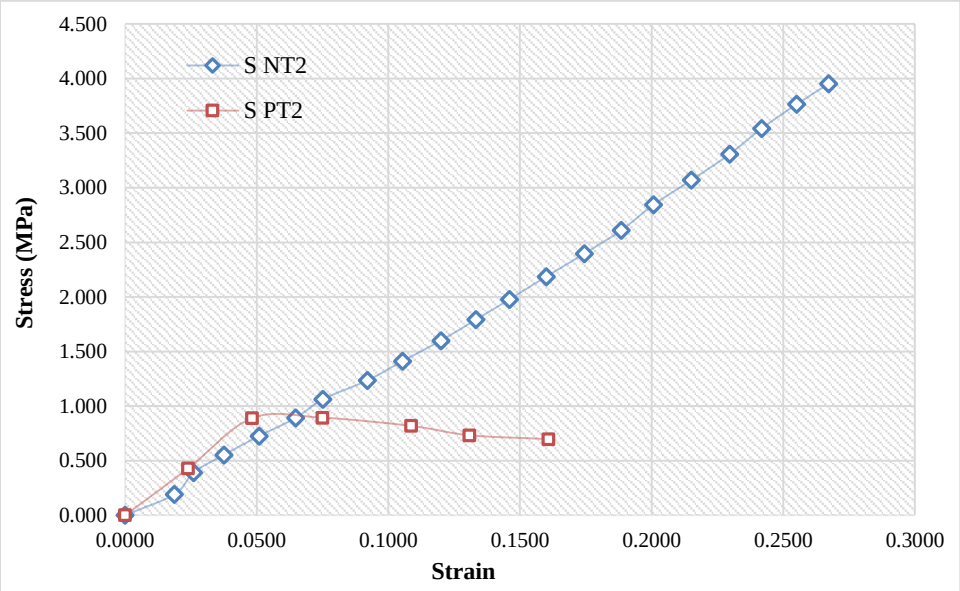

Figure 11. Stress–strain trending in the scope of manufacturing tamping orient effect

3.3. Aspect Ratio Effect

In any construction materials, the aspect ratio of dimension related to the tested specimens affect the compression strength. The compressive strength decreased from 3.8 MPa to 2.807 MPa as the aspect ratio doubled. The same observation indicated that for both loading modes, the reduction rates were 0.74 and 0.84 for normal and parallel loading modes, respectively, as listed in Table 3. Figures 12 and 13 show the stress–strain trend in the scope of the aspect ratio effect for normal and parallel loading modes, respectively.

Table 3. Aspect ratio effect on compressive strength

No.	Specimen Designation	Aspect ratio	MST	Loading method	Comp. strength, MPa	Aspect ratio effect
1	SNT2	1	II	Normal	3.80	0.74
2	PNT2	2			2.807	
3	SPT2	1		Parallel	0.893	0.84
4	PPT2	2			0.753	

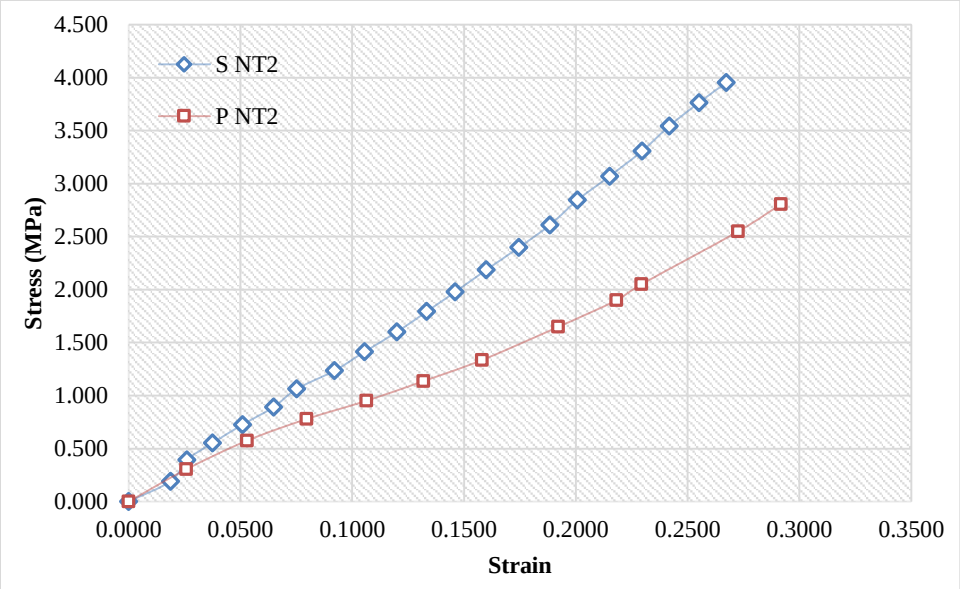

Figure 12. Stress–strain trending in the scope of aspect ratio effect in the normal loading mode

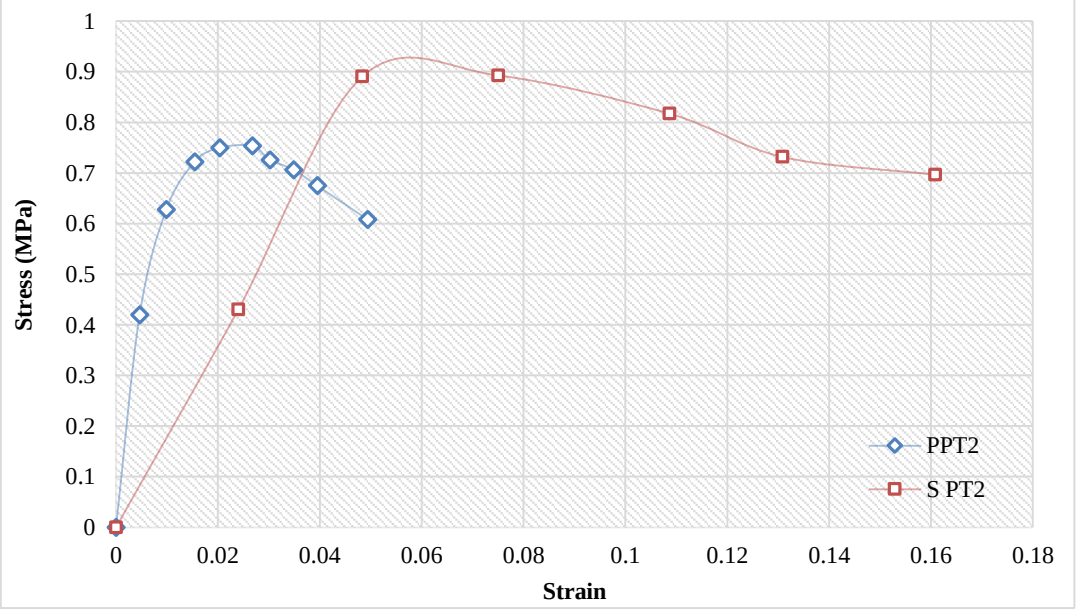

Figure 13. Stress–strain trending in scope of aspect ratio effect in the parallel loading mode

4. Failure Modes

Under compression loading, the deformed bonds across the concrete tamping layers within the section were more pronounced in loading mode 2 than that in loading mode 1. Thus, two different failure modes have been assigned as shown in Figure 14. The first is related to the first loading method, which is distinguished by developing a crushing layer across the section because of the crushing of the bonding structure under compressive stresses. The specimens tested by second loading fashion failed as the buckled bands of discrete plates. This mode of failure could be attributed to bond separation because of the developed shear stress between layers previous to buckling, and the specimens of aspect ratio (2) assigned buckling trending observed. The specimens under bending produced numerous micro-cracks after small movements. These micro-cracks might be recrystallized during the reaction of free lime, thereby effectively

self-healing the affected region. With a large movement, the flexural failure mode distinguished by the main crack continued until failure with the absence of any secondary cracks. Figure 15 confirmed the brittleness challenge of the developed matrix.

(Mode 1) **(Mode 2)**

Figure 14. Fiber-oriented effect on failure mode

(a) Front side view

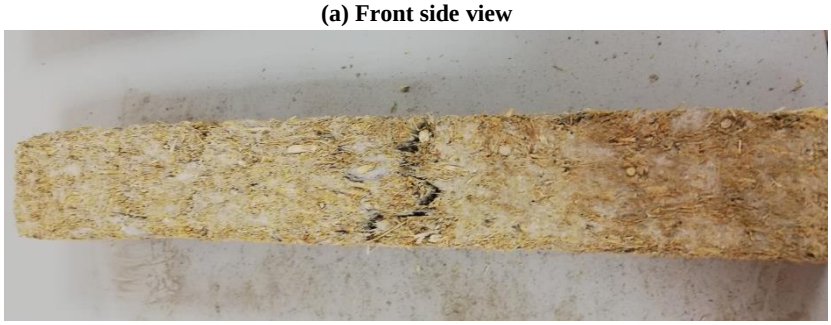

(b) Base side view

Figure 15. Flexural mode configuration of prism specimens distinguished with the main crack

5. Proposed Strawcrete Vs. Customary Hempcrete

The mechanical properties of the developed strawcrete had been compared with those of customary hempcrete blocks made from a mixture of lime and hemp shives, which were investigated by Elfordy [25] and manufactured via projection of mixture of 34% of a lime-based binder (70% of hydrate lime, 15% of pozzolanic material, and 15% of hydraulic binder), 16% hemp shives, and 50% water. Table 4 summarizes the specified samples of corresponding properties of investigated hempcrete for comparison with those presented in the results of the current study. The analysis confirmed the high similarity of elasticity response of strawcrete with that of customary hempcrete. Strawcrete showed positive improvement of gained compressive strength, extended to 1.8 for MST I against 0.18 MPa for the same mixing technique, MST I, and Young's modulus. The highest-achieved compressive strength predicated in strawcrete was 3.8 MPa for MST II, whereas the developed flexural strength (0.69 MPa) was slightly lower than that of hempcrete (0.832 MPa).

Table 4. Developed strawcrete versus hempcrete and Arbolit mechanical property comparison

Material	Mixing Technique	Density, kg/m^3	Young's modulus, MPa	Compressive strength, MPa	Flexural strength, MPa
Hempcrete [25]	Projection process, based on MST-I	291	7	0.18	-
		389	10	0.425	-
		434	12.1	0.48	0.832
Developed Strawcrete	MST-I	645	7.1	1.8	0.22
	MST-II	734	10	3.8	0.69

The best weight reduction assigned in hempcrete has a density of less than 1, and the developed strawcrete density varies between 645 and 734 kg/m^3 for the different mixing techniques. However, the assigned densities could be enhanced in consideration of the strawcrete classified as a lightweight construction material.

6. Conclusions

The experimental test results of the developed bio-composite matrix made of straw fiber as a replacement to hemp shives show that strawcrete is a renewable sustainable lightweight construction material and a proper alternative to hempcrete. Depending on these results, the elementary related conclusions were as follows:

- MST-II was assigned as the most efficient proper technique for the same loading orientation (normal to tamping layers). The compression strength of specimens prepared via MST-II was 3.8 MPa (for SNT2) against 1.8 MPa (for SNT1), which was prepared by MST-I.
- The normal loading mode was assigned as excellent mode to utilize the full strength capacity of developed matrix. For the same sequence technique, the compression strength dropped from 3.8 MPa to 0.9 MPa as the loading mode changed from normal to parallel one.
- For various mixing techniques or fiber orientations, high-strength specimens exhibited a softening behavior assigned by the modulus of elasticity dropping, whereas the specimen's compressibility indicated by Poisson ratios confirmed that fiber orientation mode 1 as the matrix of high compressibility.
- The assigned negative Poisson ratio could be affected by the large out-of-plane buckled layers within the matrix of tamping layers orientation 2. The modulus of elasticity increased as the Poisson ratio decreased and resulted in extreme anisotropy.
- For any construction materials, the aspect ratio of dimension related to tested specimens affected their compression strength. For loading mode 1, the compressive strength decreased from 3.8 MPa to 2.807 MPa as the aspect ratio doubled.
- Two different failure modes were assigned for the compressive failure trend. The first related to the first loading mode was distinguished by developing a crushing layer across the section, whereas the specimens tested by the second loading mode failed as buckled bands of discrete plates. The specimens with aspect ratio (2) assigned buckling trend were clearly observed. With a large movement, flexural failure mode distinguished by the main crack continued until failure with the absence of any secondary cracks, which were confirmed by the brittleness challenge of the developed matrix.
- Analysis of the developed strawcrete versus the hempcrete confirmed the high similarity of elasticity response of strawcrete with that of customary hempcrete. Strawcrete showed positive improvement of enhanced compressive strength, which was extended to 1.8 MPa for MST-I against 0.18 MPa for the same mixing technique.

7. Conflicts of Interest

The authors declare no conflict of interest.

8. References

[1] Williams, Joseph, Mike Lawrence, and Pete Walker. "A Method for the Assessment of the Internal Structure of Bio-Aggregate Concretes." Construction and Building Materials 116 (July 2016): 45–51. doi:10.1016/j.conbuildmat.2016.04.088.

[2] Mukherjee, Agnita, and Colin MacDougall. "Structural Benefits of Hempcrete Infill in Timber Stud Walls." International Journal of Sustainable Building Technology and Urban Development 4, no. 4 (December 2013): 295–305. doi:10.1080/2093761x.2013.834280.

[3] Dai, Dasong, and Mizi Fan. "Preparation of Bio-Composite from Wood Sawdust and Gypsum." Industrial Crops and Products 74 (November 2015): 417–424. doi:10.1016/j.indcrop.2015.05.036.

[4] Hornby, Rachelle. "A Review of Alternative Building Materials in comparison to CMU: Hempcrete, Woodcrete, Papercrete." (2017).

[5] Udawattha, Chameera, and Rangika Halwatura. "Thermal Performance and Structural Cooling Analysis of Brick, Cement Block, and Mud Concrete Block." Advances in Building Energy Research 12, no. 2 (November 25, 2016): 150–163. doi:10.1080/17512549.2016.1257438.

[6] Bedlivá, Hana, and Nigel Isaacs. "Hempcrete – An Environmentally Friendly Material?" Advanced Materials Research 1041 (October 2014): 83–86. doi:10.4028/www.scientific.net/amr.1041.83.

[7] Jami, Tarun, Deepak Rawtani, and Yadendra K. Agrawal. "Hemp Concrete: Carbon-Negative Construction." Emerging Materials Research 5, no. 2 (December 2016): 240–247. doi:10.1680/jemmr.16.00122.

[8] Jami, Tarun, S.R. Karade, and L.P. Singh. "A Review of the Properties of Hemp Concrete for Green Building Applications." Journal of Cleaner Production 239 (December 2019): 117852. doi:10.1016/j.jclepro.2019.117852.

[9] Hirst, Edward A. J., Peter Walker, Kevin A. Paine, and Tim Yates. "Characteristics of Low-Density Hemp-Lime Building Materials." Proceedings of the Institution of Civil Engineers - Construction Materials 165, no. 1 (February 2012): 15–23. doi:10.1680/coma.1000021.

[10] Walker, R., and S. Pavía. "Moisture Transfer and Thermal Properties of Hemp–lime Concretes." Construction and Building Materials 64 (August 2014): 270–276. doi:10.1016/j.conbuildmat.2014.04.081.

[11] Pietruszka, B, M Gołębiewski, and P Lisowski. "Characterization of Hemp-Lime Bio-Composite." IOP Conference Series: Earth and Environmental Science 290 (June 21, 2019): 012027. doi:10.1088/1755-1315/290/1/012027.

[12] Nguyen, Tai Thu, Vincent Picandet, Patrick Carre, Thibaut Lecompte, Sofiane Amziane, and Christophe Baley. "Effect of Compaction on Mechanical and Thermal Properties of Hemp Concrete." European Journal of Environmental and Civil Engineering 14, no. 5 (May 16, 2010): 545–560. doi:10.3166/ejece.14.545-560.

[13] Magwood, Chris. Essential Hempcrete Construction: The Complete Step-by-Step Guide. New Society Publishers, 2016.

[14] Aigbomian, Eboziegbe Patrick, and Mizi Fan. "Development of Wood-Crete Building Materials from Sawdust and Waste Paper." Construction and Building Materials 40 (March 2013): 361–366. doi:10.1016/j.conbuildmat.2012.11.018.

[15] Williams, Joseph, Mike Lawrence, and Pete Walker. "The Influence of Constituents on the Properties of the Bio-Aggregate Composite Hemp-Lime." Construction and Building Materials 159 (January 2018): 9–17. doi:10.1016/j.conbuildmat.2017.10.109.

[16] Chabannes, Morgan, Jean-Charles Bénézet, Laurent Clerc, and Eric Garcia-Diaz. "Use of Raw Rice Husk as Natural Aggregate in a Lightweight Insulating Concrete: An Innovative Application." Construction and Building Materials 70 (November 2014): 428–438. doi:10.1016/j.conbuildmat.2014.07.025.

[17] Yin, Xunzhi, Mike Lawrence, Daniel Maskell, and Wen-Shao Chang. "Construction and Monitoring of Experimental Straw Bale Building in Northeast China." Construction and Building Materials 183 (September 2018): 46–57. doi:10.1016/j.conbuildmat.2018.05.283.

[18] Ewaid, Salam, Salwan Abed, and Nadhir Al-Ansari. "Water Footprint of Wheat in Iraq." Water 11, no. 3 (March 14, 2019): 535. doi:10.3390/w11030535.

[19] Stevulova, N., L. Kidalova, J. Junak, J. Cigasova, and E. Terpakova. "Effect of Hemp Shive Sizes on Mechanical Properties of Lightweight Fibrous Composites." Procedia Engineering 42 (2012): 496–500. doi:10.1016/j.proeng.2012.07.441.

[20] Caporale, Andrea, Fulvio Parisi, Domenico Asprone, Raimondo Luciano, and Andrea Prota. "Comparative Micromechanical Assessment of Adobe and Clay Brick Masonry Assemblages Based on Experimental Data Sets." Composite Structures 120 (February 2015): 208–220. doi:10.1016/j.compstruct.2014.09.046.

[21] British Standards Institution, BS 890:1995; Specification for building limes.

[22] Iraqi Specification No. 5, (1984), "Portland Cement", Baghdad, Iraq.

[23] American Society of Testing and Material (2003). "Standard Test Method for Time of Setting of Hydraulic Cement by Vicat Needle". ASTM C-191, (2003); West Conshohocken, PA.

[24] William Stanwix and Alex Sparrow,"The hempcrete book; Designing and building with hemp-lime" Published by Green Books; (2014).

[25] Elfordy, S., F. Lucas, F. Tancret, Y. Scudeller, and L. Goudet. "Mechanical and Thermal Properties of Lime and Hemp Concrete ('hempcrete') Manufactured by a Projection Process." Construction and Building Materials 22, no. 10 (October 2008): 2116–2123. doi:10.1016/j.conbuildmat.2007.07.016.